

# Identification of Nonlinear System for Elastically Supported Cylinder on Cross-Flow Using Wavelet Transform

SubektiSubekti<sup>a,c</sup>, HarusLaksanaGuntur<sup>b,\*</sup>, Vivien S. Djanali<sup>b</sup>, AchmadSyaifudin<sup>b</sup>

<sup>a</sup>Graduate Program of Engineering Department, Faculty of Industrial and Technology, Institut Teknologi Sepuluh Nopember, Kampus ITS Sukolilo, Surabaya, 60111, Indonesia

<sup>b</sup>Mechanical Engineering Department, Faculty of Industrial and Technology, Institut Teknologi Sepuluh Nopember, Kampus ITS Sukolilo, Surabaya, 60111, Indonesia

<sup>c</sup>Mechanical Engineering Department, Faculty of Industrial, Universitas Mercu Buana, Jl. Meruya Selatan No. 1, Kembangan, Jakarta, 11650, Indonesia

Received 6 Aug 2023

Accepted 10 Jan 2024

## Abstract

This study investigates an application of the wavelet transform to identify the characteristics of a nonlinear system of an elastically supported cylinder in cross-flow under uniform airflow. The envelope of the time response and instantaneous frequency is extracted using the wavelet transform to identify the nonlinear characteristics of the system. Responses within the range of the lock-in and nonlinear jump phenomena were investigated. Flow-induced vibration in a cylinder supported by two beams shows that the wavelet transform can identify the lock-in phenomena in both forward-sweep and backwards-sweep experiments. The study shows that the vibration phenomenon caused by a flow in a beam supported cylinder medium with forward-sweep and backwards-sweep does not affect the damping characteristic due to the stiffness. The result will be beneficial in controlling vibration effect.

© 2024 Jordan Journal of Mechanical and Industrial Engineering. All rights reserved

**Keywords:** wavelet transform; nonlinear; flow-induced vibration; lock-in; forward-sweep; backwards-sweep; identification.

## 1. Introduction

Vibrations induced by a structure flow are dynamically interacting systems that incorporate forces on the structure caused by the surrounding fluid. The fluid forces could deform the structure. It is called vibration because of the flow or vibration induced by the flow. Flow-induced structural vibrations have been found in areas of aerospace industry, turbine blades, heat exchanger tubes, nuclear reactor components, and energy converters on recent advances in physics insights and modelling of flexible cylindrical flow-induced vibrations (FIVs) [1 - 5]. Flow-induced vibrations (FIVs) of circular cylinders potentially lead to some negative consequences (e.g., structural damage due to fatigue) or positive consequences (e.g., vibrate the wind/hydro energy harvesting) [6,7,8].

The elastically supported structure lies in the cross-flow that produces vibrations caused by the flow due to the vortex around structures. The vortex shedding frequency approaches the natural structural frequency, so a lock-in phenomenon and vibration of large amplitudes occur. It is a kind of self-awakening vibration [9 -14]. The phenomenon of flow-induced vibration is not only a characteristic of the time domain but also the frequency domain. The power spectrum of the Fourier Transform analysis aims to investigate the frequency characteristics

of flow-induced vibrational phenomena. However, the Fourier transformation method where the signal is not widespread in the time and frequency domain, is ineffective, and the frequency analysis using ordinal Fourier transformation is not suited for flow-induced vibration analysis because it is not a linear phenomenon, and the oscillation mechanism can change dynamically with time. Therefore, time-frequency analysis based on wavelet transformations is preferred to identify nonlinear characteristics of elastically supported structures in cross-flow. The wavelet transformation is a spectrum of Fourier transformations locating a time window on non-stationary data. It is because wavelet transformation transforms a signal to the base form of a wavelet by shifting and scaling it so that the value of the multiscale wavelet coefficient is based on the high-resolution wavelet coefficient [15, 16]. A comprehensive overview of flow-induced vibration and wavelet transformations is found in many publications. A comparison between the wake response for single fixed and single row and free to vibrate was performed using Fourier Transform and Wavelet Transformation [17 -19]. Wavelet analysis showed that the frequency modulated amplitude in time, and the second and third pitch wavelet spectra contained high energy events along with the sporadic distribution of low energy events without the phenomenon of mode switching [20]. A wavelet transforms application in the flow vibrations analyses

\* Corresponding author e-mail: haruslg@me.its.ac.id.

induced from a cylinder in cross flow. They show that the wavelet transformations apply to stationary and non-stationary processes [21 - 24]. The main point of their research is that the detailed use of wavelet transformations can provide valuable diagnostic information for coronal seismology. Spectral analysis using Fourier transforms on all-time series could not identify the characteristics of the bistable flow phenomenon. The Wavelet transformation, however, is a very proper tool. This case explains each time-dependent intermittent phenomenon based on a non-stationary series [25 - 27]. Investigation of the effect of Reynolds' numbers on flow interference between two side-by-side stationary cylinders and associated flow-induced forces using the finite element method and wavelet analysis [28]. This wavelet precisely reconstructs various signals in different situations, such as upstream, downstream, and around the bluff body (cylinder) [29 - 40]. However, wavelet analysis cannot identify modal parameters and investigate the characteristics of flow-induced vibrations. These shortcomings that prompted us to conduct this study. The parameter model identified with the envelopes and instantaneous wavelet methods by applying the function of the wavelet-based envelope modulates vibration signals [41 - 48]. This envelope extracts the signal envelope. The results showed that the Continuous Wavelet Transform (CWT) signal jointly established modal extraction and signal sheaths to estimate the damping ratio. Wavelet transformation is a method to analyze combined time-frequency of nonstationary signals. Estimation of the capital parameters of the vibrating system used wavelet transformations [49 - 53]. For the instantaneous nature of the transient response, the ridge of the wavelet transformation can be used to reconstruct the skeletal curve and identify the capital parameters of a system [54]. A technique developed to identify the characteristics of nonlinear systems by comparing extraction results uses wavelet analysis and Hilbert transformations (HT) [55]. Wavelet can analyze the envelope and instantaneous frequency of shifting signals. In addition, the result showed less noise compared to Hilbert's technique. Wavelet Packet Decompose (WPD) application for modal analysis of circular cylinders is supported by two elastic cantilever beams and wire [56]. Vibration testing at the Vibration Laboratory of Mercubuana University has been carried out on construction and vehicle systems, among others, to determine the effect of heaving and pitching on ship motion due to spring bending moments [57 - 64]. Regarding vibration that occurs in industrial application, the problem of cracking due to density curve is a concern thus based on the research that had been carried out, vibration fatigue analysis must be carried out to prevent cracking based on the material density toleration [65-73]. Instantaneous pressure signals are irregular at low vibrational frequencies but become more regular with increasing frequencies in pressure profiles, periodicity, and wave transformation parameters [74]. Effects of different geometric configurations of slat and flap on aeroacoustics time frequency are characteristics of experimental measurements and wavelet analysis [75].

This study presents experimental results of elastically supported cylinders excited by lift forces that cause the cylinder to vibrate in a perpendicular direction to fluid

flow (i.e., cross-flow vibrations). The envelope of instantaneous time and frequency response is extracted using wavelet transformations. Experimental settings and procedures are outlined, provides detailed mechanical models of the system and explains the theoretical foundations of wavelet theory in part 2, while the results and discussion are presented in Part 3. Finally, the study presents the conclusion in part 4.

## 2. Material and Method

The cylinder is supported by two clamped beams, and a wire is presented in Figure 1. A round plate with a small hole is equipped in the center of the cylinder. There is a slight gap between the wire and the cylinder. The beams are placed outside the wind tunnel testing area to avoid interruption of airflow. For uniform airflow configurations, a test is performed as flow velocities varying from 0.6 to 4.1 m/s and from 4.1 to 0.6 m/s, which are called forward and reverse sweeps, respectively. Experimental studies were conducted in open wind tunnels with a square cross-section of 30 cm × 30 cm. Airflow is generated from centrifugal fans. From the fan, air passes through a chamber containing a series of sails and honeycombs to straighten the flow and reduce turbulence. The test cylinder is a polycarbonate tube with an outer diameter of cross-section  $D = 0.045$  m, length  $L = 0.32$  m, and mass  $m = 0.06642$  kg. The beam is made of stainless steel with a length of 0.185 m, a height of 0.03 m, and a thickness of 0.006 m, and it has a Young modulus of 206 GPa. The wire material is SWP-A with Young's modulus of 208.1 GPa, a tensile strength of 1600 MPa, and a diameter of 0.55 mm. The diameter of the hole in the round plate is 3 mm, and voltage is applied in the wire at one end. The other end is clamped to maintain a constant load.

In the case of elastically supported cylinders, the cylinders will vibrate at a definite frequency due to tensile and lift forces. The drag force will excite the cylinder in the direction of fluid flow (in-line vibration). However, the lift force will vibrate the cylinder in a direction perpendicular to the direction of fluid flow (cross-flow vibration). In the experimental setting of this study, cross-flow vibrations were dominant.

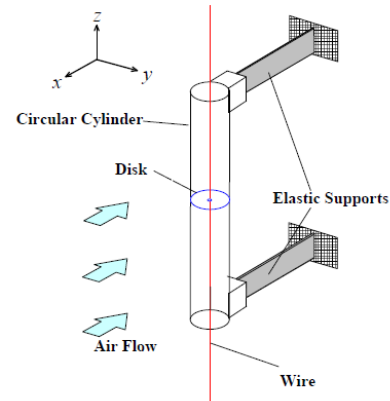


Figure 1. Elastically supported cylinder with wire.

Figure 2 shows a schematic diagram of the measurement system. The vibration responses of cylinders and beams are measured with two laser displacement sensors (LB040/LB-1000, Keyence Corp.). The output

signal of the laser displacement sensor is acquired from the FFT Analyzer (CF3600, OnoSokki.). Anemometer (HP-866B-APP) is used to measure flow velocity.

For this study, the elastically supported cylinder was modelled as a Single Degree of Freedom (SDOF) system, as shown in Figure 3. A cylinder of mass  $m$  is supported by two elastic beams with spring constant,  $k_L$  and viscous damping coefficient,  $c_L$ . A round plate with a small hole is allowed in the center of the cylinder. A wire with a nonlinear stiffness function,  $k_N$  and a viscous damping coefficient,  $c_w$  passes through the hole so that there is a chink denoted by  $x_0$  between the wire and the plate hole. At the same time the relative displacement between the cylinder and the wire is lower than  $x_0$ , the system will be a linear structure. When the relative displacement is higher than  $x_0$ , i.e.,  $|y - x| \geq x_0$ , a nonlinear effect will appear on the structure due to the nonlinear spring nature of the wire. The equation of motion of the system is described as follows:

$$\text{When } |y - x| < x_0, \quad m\ddot{y} + c_L\dot{y} + k_L y = F(t), \quad (1.a)$$

$$\text{When } |y - x| \geq x_0, \quad m\ddot{y} + c_L\dot{y} + k_L y + c_w\dot{x} + k_N(x) = F(t). \quad (1.b)$$

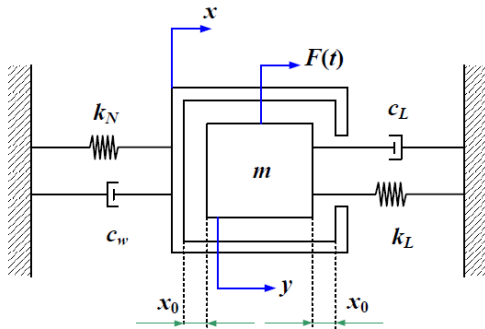


Figure 3. Single degree of freedom system.

The nonlinear stiffness of the system is expressed as  $k_N(x) = k_{wl}x + k_{wN}x^3$ . (2)

Replace equations. (2) into Equation. (1. b) we get  $m\ddot{y} + c_L\dot{y} + k_L y + c_w\dot{x} + k_{wl}x + k_{wN}x^3 = F(t)$ , (3)

that  $x$  is the wire displacement,  $y$  is the cylinder displacement, and  $k_{wl}$  and  $k_{wN}$  are the spring constants for linear and nonlinear properties, respectively. An external force is applied with  $F(t)$ . Furthermore, collisions between the displacements of  $x$  and  $y$  occur when  $y = x - x_0$  or  $y = x + x_0$  for the equation (3), which can be formulated as follow:

$$m\ddot{x} + c_L\dot{x} + k_L(x \pm x_0) + c_w\dot{x} + k_{wl}x + k_{wN}x^3 = F(t), \quad (4)$$

In the case of negligible values  $x_0$ , we can analyze the above Equation taking into account the fundamental components of harmonics as follows:

$$x = X \sin(\omega t), \text{ and } F(t) = F_0 \sin(\omega t + \phi). \quad (5)$$

$$\begin{aligned} \text{Replace equations (5) into the equation (4) we get} \\ -m\omega^2 X \sin(\omega t) + (c_w + c_L)\omega X \cos(\omega t) \\ + (k_L + k_{wl})X \sin(\omega t) \\ + k_{wN}X^3 \left\{ \frac{3}{4} \sin(\omega t) + \frac{1}{4} \sin(3\omega t) \right\} \\ = F_0 \sin(\omega t) \cos(\phi) - F_0 \cos(\omega t) \sin(\phi) \end{aligned} \quad (6)$$

Equating the coefficients  $\sin(\omega t)$  and  $\cos(\omega t)$  (fundamental component) yields

$$-m\omega^2 X + (k_L + k_{wl})X + \frac{3}{4}k_{wN}X^3 = F_0 \cos(\phi) \quad (7)$$

$$\text{And} \\ (c_w + c_L)\omega X = -F_0 \sin(\phi), \text{ each} \quad (8)$$

The magnitude of the response and phase are determined as

$$\left| \frac{X}{F_0} \right| = \frac{1}{\left[ \left\{ -m\omega^2 + (k_L + k_{wl}) + \frac{3}{4}k_{wN}X^2 \right\}^2 + (c_w + c_L)^2 \omega^2 \right]^{1/2}} \quad (9)$$

$$\phi = \tan^{-1} \left( \frac{1}{\left( m\omega^2 + (k_L + k_{wl}) + \frac{3}{4}k_{wN}X^2 \right)} \right), \quad (10)$$

Let's rewrite the forced vibration equation for SDOF as  $\ddot{y} + 2h_0(A)\dot{y} + \omega_0^2(A)y = \frac{F(t)}{m}$ , (11) which  $h_0$  and  $\omega_0^2$  are symmetrical viscous damping and system rigidity, respectively, which depend on the amplitude (A). According to the main properties of HT, equation (11) can be converted by HT to the following analytical signals:

$$\ddot{Y} + 2h_0(A)\dot{Y} + \omega_0^2(A)Y = \frac{F}{m}, \quad (12)$$

$$\text{which} \\ Y(t) = y(t) + j\tilde{y}(t) = A(t)e^{i\theta(t)}, \quad (13)$$

$A(t)$  is the instantaneous magnitude or envelope,  $\theta(t)$  is the instantaneous phase, and  $\tilde{y}(t)$  is HT of response signal  $y(t)$  obtained as:

$$\tilde{y} = \frac{1}{\pi} \rho v \int_{-\infty}^{+\infty} \frac{y(\tau)}{t - \tau} d\tau, \quad (14)$$

$\rho v$  indicates the main value of Cauchy. The instantaneous frequency  $\omega(t)$  is defined as  $\omega(t) = \dot{\theta}(t)$ . (15)

$$\text{Two derivatives of } Y(t) \text{ are obtained as} \\ \dot{Y}(t) = Y(t) \left[ \frac{\dot{A}(t)}{A(t)} + i\omega(t) \right], \quad (16)$$

$$\ddot{Y}(t) = Y(t) \left[ \frac{\ddot{A}(t)}{A(t)} - \omega^2(t) + 2i \frac{\dot{A}(t)\omega(t)}{A(t)} + i\dot{\omega}(t) \right]. \quad (17)$$

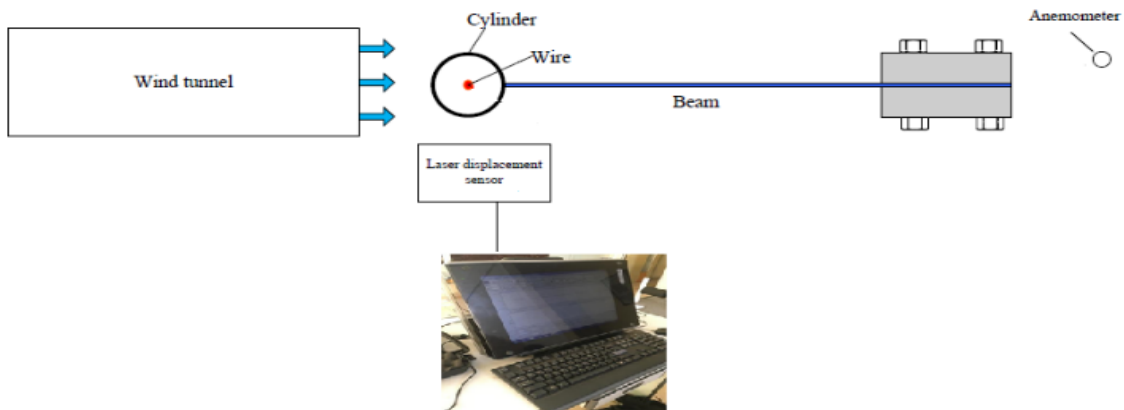


Figure 2. Schematic diagram of the measurement system.

By replacing equations (16) and (17) into the Equation. (12), we obtain a representation of the corresponding capital parameters as follows:

$$Y \left[ \frac{\ddot{A}}{A} - \omega^2 + \omega_0^2 + 2h_0 \frac{\dot{A}}{A} + i \left( 2 \frac{\dot{A}\omega}{A} + \dot{\omega} + 2h_0\omega \right) \right] = \frac{\ddot{F}}{m}. \quad (18)$$

To solve two equations for the real and imaginary parts of the equation (18), the expression for a modal parameter is written as below:

$$\omega_0^2(t) = \omega^2 + \frac{\alpha(t)}{m} - \frac{\beta(t)A}{A\omega m} - \frac{\ddot{A}}{A} + \frac{2\dot{A}^2}{A^2} + \frac{\dot{A}\dot{\omega}}{A\omega}, \quad (19)$$

$$h_0(t) = \frac{\beta(t)}{2\omega m} - \frac{\dot{A}}{A} - \frac{\dot{\omega}}{2\omega}, \quad (20)$$

which

$$\frac{\alpha(t)}{m} = \frac{\ddot{A}}{A} - \omega^2 + \omega_0^2 + 2h_0 \frac{\dot{A}}{A}, \quad (21)$$

$$\frac{\beta(t)}{m} = 2 \frac{\dot{A}}{A} + \dot{\omega} + 2h_0\omega. \quad (22)$$

Once  $h_0(A)$  and  $\omega_0^2(A)$  are known, the damping and string characteristics of  $f_d(A)$  and  $f_s(A)$  are proportional, and each can be obtained through following equation

$$f_d(A) = 2\dot{A}h_0(A) \text{ and} \quad (23)$$

$$f_s(A) = A\omega_0^2(A). \quad (24)$$

This approach is also discussed in detail in [76].

The wavelet transform has been widely used because it can present time-frequency (time-scale) signals better than the short-time Fourier transform. The wavelet transform uses a variable window width, wide at low frequencies and narrows at high frequencies. Therefore, it is possible to analyze data with short-duration basis functions to measure the high-frequency components. The advantage of wavelet analysis is that it is able to analyze data in different frequency components and represent them with scale-adjusted resolution [48].

A wavelet is a family of functions generated by a wavelet basis function  $\psi(x)$ , known as the parent wavelet function having a scale factor,  $a$  and translation,  $b$ . The parent wavelet function is defined as

$$\Psi_{a,b}(t) = \frac{1}{\sqrt{|a|}} \psi \left( \frac{t-b}{a} \right). \quad (25)$$

A CWT is a wavelet transform to analyze non-stationary signals that change over time. It can perform local analysis with a window on the signal as low as possible. The CWT can be formulated as follows:

$$CWT(b, a) = \frac{1}{\sqrt{a}} \int_{-\infty}^{\infty} x(t) \psi^* \left( \frac{t-b}{a} \right) dt. \quad (26)$$

CWT is a continuous signal function that generates wavelet coefficients, defined as the sum of the multiplied signals of the wavelet function  $\psi$  scaled by  $a$  and translated by  $b$  across the time domain. Information about frequency and time is indicated by the scale and translation, respectively.

The normalization factor  $\frac{1}{\sqrt{a}}$  is applied to ensure that the resulting energy is the same for all values of  $a$ . If  $a > 1$ , then the Wavelet Function  $\psi$  will be stretched along the time axis, and if  $0 < a < 1$ , then the Wavelet Function will be compressed.

The function  $\psi(t)$  satisfies the conditions for an oscillatory functional with fast decay to zero, zero mean value, normalization, and acceptance as follows:

$$\int_{-\infty}^{+\infty} \psi(t) dt = 0 \text{ or } \int_{-\infty}^{+\infty} |\psi(t)|^2 dt = 1, \quad (27)$$

and

$$\int_{-\infty}^{\infty} \frac{|\hat{\psi}(\omega)|^2}{|\omega|} d\omega < \infty, \quad (28)$$

which  $\hat{\psi}(\omega)$  Fourier Transforms of  $\psi(t)$ . The selection of an appropriate Wavelet Function or a parent depends on the type of signal information required. Therefore, when

we use wavelets for identification, the identified curve must be adapted to be similar to the original signal. Several different analytic functions have been used for wavelet analysis; one of them is the complex Shannon wavelet analysis.

It is obtained from the complex frequency of the B-spline wavelet by setting  $m$  to 1 and is defined as

$$\psi(x) = \sqrt{f_b} \text{sinc}(f_b) e^{2i\pi f_c x}. \quad (29)$$

A complex Shannon wavelet is a set of complex sinusoidal in the envelope of the sinc function, where the center frequency parameter  $f_c$  and the bandwidth parameter  $f_b$  control the width of the main lobe of the sinc function [77].

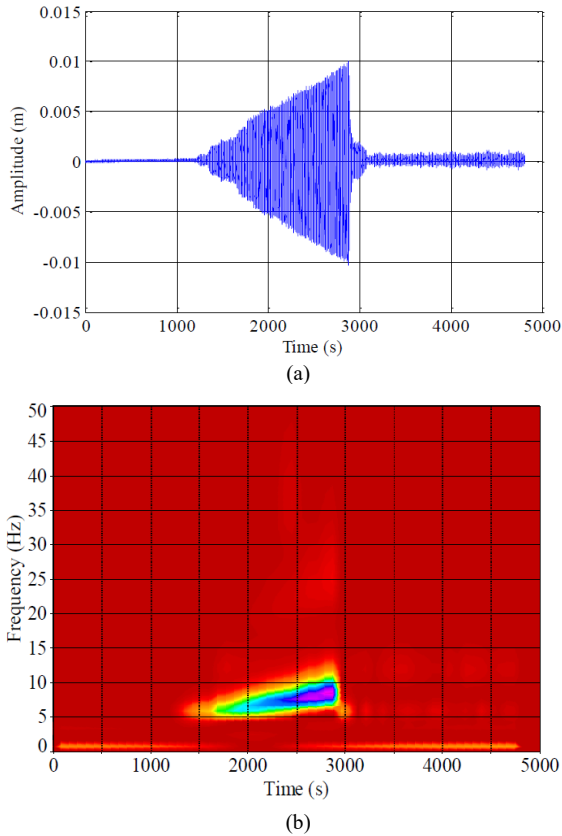
Both the instantaneous frequency and envelope of the wavelet transform are used in this study. The method of estimating parameters using instant frequency is known as wavelet ridge analysis while the one using envelope is a wavelet skeleton analysis. The Wavelet Transform of  $x(t)$  is an expansion of the function  $x(t)$  as a basis for the function  $\psi(t)$  constructed from the dilation and translation of the parent wavelet, Eq. (11). This signals class is asymptotic and support the analysis of the time-frequency signals [78-89].

### 3. Result and Discussion

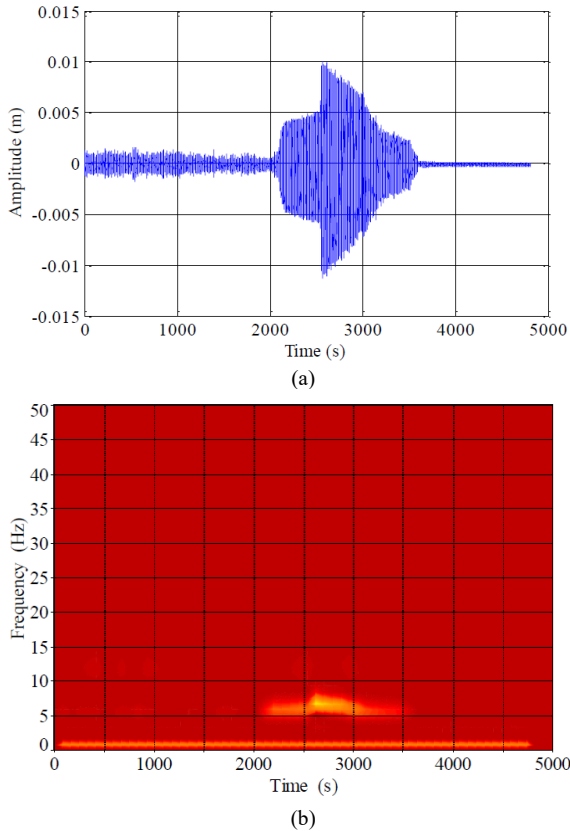
Experiments involving the static case were conducted to determine the effect of wire tension on the system. It was to define the degree of strain on the wire used in the dynamic experiments. An impulse excitation was applied to the middle of the cylinder, while the response of the cylinder was measured with a laser displacement sensor. We used a 4 N tension on the wire for our experiment to study the effect of geometric nonlinearity.

The experiment was conducted using a wind tunnel where the airflow velocity was varied gradually from 0.6 to 4.1 m/s (forward sweep) and from 4.1 to 0.6 m/s (backward sweep). The Reynolds number range is approximately  $6.12 \times 10^3 < Re < 3.78 \times 10^4$ . The wavelet transform provides a method for determining the envelope and instantaneous frequency of the signals in figures 5 and 6. The wavelet had no frequency parameter. Instead, it had a scale parameter that could be used to determine frequency. The modulus and phase of the complex Shannon wavelet could be used to extract the envelope and instantaneous frequency.

Figure 4 shows the response of the cylinder in the forward sweep. When the flow velocity is slow, the vibration amplitude of the cylinder is almost constant. However, the vibration amplitude increases dramatically after 1300 seconds as the vortex shedding frequency approaches the natural frequency of the structure. When the flow velocity becomes fast enough, the amplitude decreases rapidly. In the case of linear systems, locking phenomena can occur around the natural frequency of the structure. However, the frequency lock-in of nonlinear systems increases slightly. Experiments using the same setup shown in Figure 4 were conducted for a backward sweep of the flow velocity, with results are also shown in Figure 5. The vibration amplitude of the cylinder is smaller than in figure 4. When the speed is swept backwards, the largest amplitude is found from 2125 s to 3125 s. The amplitude increases by about 2600 seconds, and then the frequency slowly decreases to 3000 seconds.



**Figure 4.** Test results under forward sweep response: (a) cylinder amplitude and (b) time-frequency analysis of the wavelet transform.



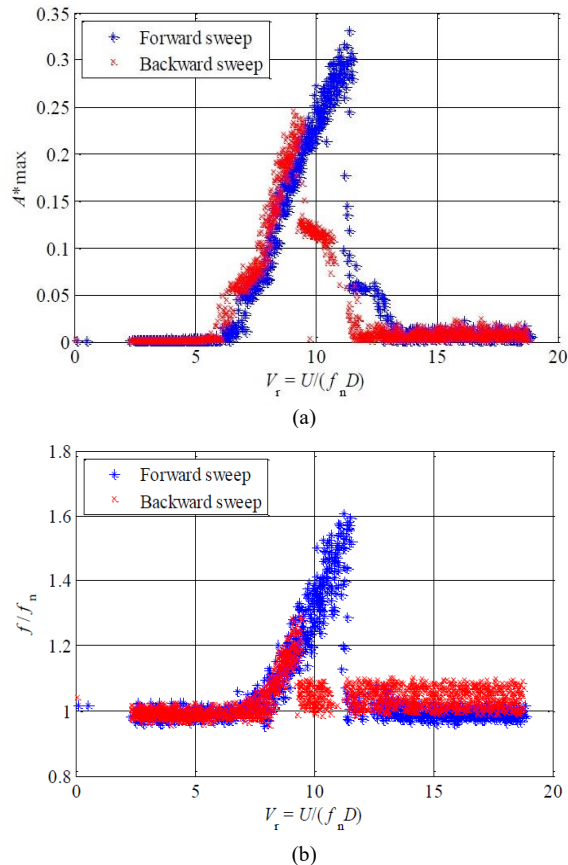
**Figure 5.** Test results under backward sweep response: (a) cylinder amplitude and (b) time-frequency analysis of the wavelet transform

Figure 6(a) shows the relationship between the reduced velocity and the non-dimensional amplitude of the cylinder motion defined as  $A_{max}^* = y_{max}/D$ . The reduced velocity is defined as  $V_r = U/(f_n D)$ . Figure 7(b) shows the relationship between velocity reduction and frequency ratio  $f/f_n$ . The vibration amplitude of the cylinder under forward sweep increases from  $V_r = 6$ . However, the frequency in Figure 6(b) does not change until  $V_r = 7$ . Here, the so-called locking phenomenon seems to occur. After this region, a geometric nonlinear response is identified in the system. The forward sweep response shows a jumping phenomenon at  $V_r = 11.9$ . The amplitude decreases by a specific value once and then decreases rapidly at approximately  $V_r = 13$ . In the backward sweep response, the vibration amplitude of the cylinder increases in two stages. The first and second increases seem to be generated by lock-in and nonlinear phenomena, respectively. A nonlinear system exhibits characteristics such as beating phenomena, complex limit-cycle behavior, phase shifts, and vortex dynamics. These features indicate the system's departure from linearity and the presence of intricate and unpredictable dynamics. Adding the nonlinear accumulation based on the frequency and amplitude between fluid and structural oscillations resulted in a more complex motion and flow field. The coupling raises the vortex-induced vibration that are difficult to model and not fully understood.

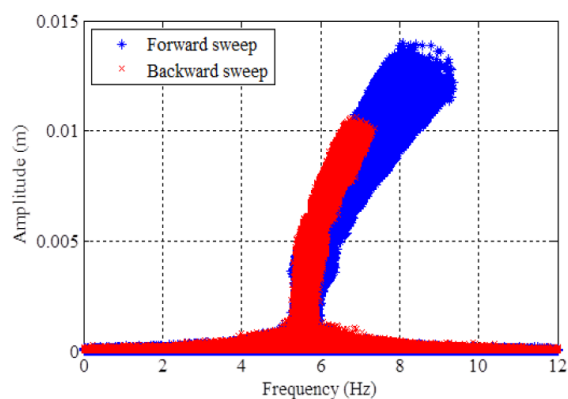
Figure 7 shows the relationship between the frequency and vibration amplitude of the system. This curve corresponds to the backbone curve of the nonlinear system. Although the front angle view of the cylinder is slightly wide, the analysis is plotted using red (forward sweep) and blue (backward sweep) dotted lines for comparison. The effective stiffness of the spring had been successfully achieved by the estimation of the frequency and amplitude which together determines the backbone curve with a minor difference between forward sweep and backward sweep in the larger amplitude. It is critical to determine the characteristics of the nonlinear restoring force as a function of the vibration amplitude. Figure 9(a) shows the restoring force curves of the forward and backward sweeps, as identified using equation (28), based on the complex Shannon wavelet. The thin line shows the curve obtained by the least squares error method. As shown in Figure 8(a), the restoring force curve of the forward sweep response shows stronger nonlinearity than the backward sweep response. The approximate characteristics of the damping force can be derived using equation (29).

Figure 8(b) shows that the estimated damping force based on the complex wavelet is a straight line following the linear damping part of the equation  $c_w = 0,08$  for both forward and backward responses. The linear spring constant  $k_L$  and viscous damping coefficient  $c_L$  were experimentally determined as 1,48 N/m and 0,1112, logarithmic decrement of free vibration, respectively. The nonlinear stiffness parameters of the extracted values were determined using curve fitting on the measured restoring force data. The nonlinear stiffness was determined to be  $k_N(x) = 5.0 \cdot 10^5 \cdot x^3 + 43 \cdot x$  for a forward sweep and  $k_N(x) = 1.8 \cdot 10^5 \cdot x^3 + 30 \cdot x$  for a backward sweep. The approximate damping force characteristics can be derived using Eq. (23). Figure 8(b) shows that the damping

force is estimated as a straight line, similar to linear damping. Then, the additional damping is estimated as  $c_w = 0,08$  for both forward and backward responses. As mentioned above, the nonlinear stiffness of forward and backward sweep shows different values. In general, the geometric nonlinearity of a structure shows similar values for the nonlinear stiffness. Therefore, this phenomenon seems to be the combined result between the geometric nonlinearity of the structures and the flow-induced vibration.



**Figure 6.** Vibration amplitude expressed in terms of cylinder diameter as a function of velocity reduction for the forward sweep and backward sweep responses of the (a) amplitude and (b) frequency responses



**Figure 7.** The backbone curve of the forward sweep and backward sweep.

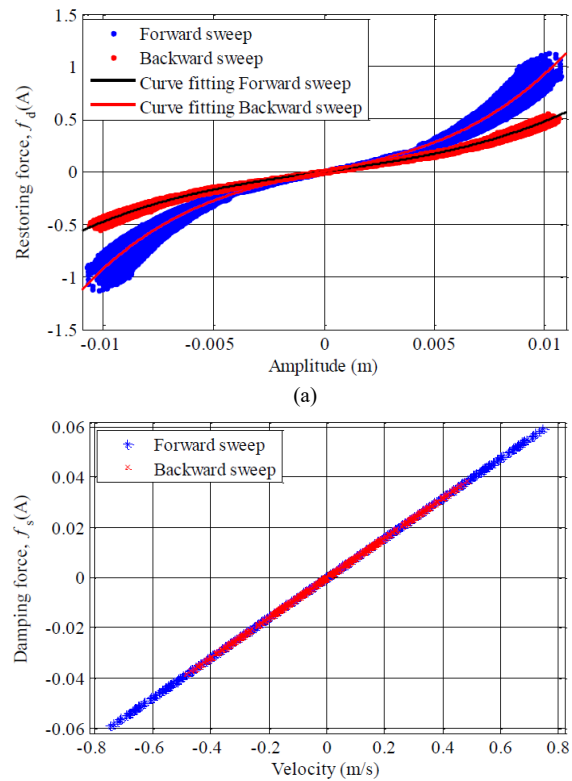


**Figure 8.** Forward sweep and reverse sweep (a) identify the spring restoring force and determine the nonlinear characteristics  $\omega_{tot}^2$ , and (b) the damping force.

#### 4. Conclusion

Flow-induced vibration in a cylinder supported by two beams shows that the wavelet transform can identify the lock-in phenomena in both forward-sweep and backwards-sweep experimental conditions. In the forward sweep condition, the amplitude and nonlinear stiffness are bigger than the backward sweep condition. Meanwhile, the damping force generated due to the influence of forward and backward sweep does not change completely. For further research, it is necessary to convert the results of the mathematical model to the experimental results.

#### Acknowledgment

Thanks to prof. Dr. Kobayashi Yukinori from Hokkaido University for permission to use the laboratory, which assists in completion of this paper.

#### References

- [1] L. Ma, K. Lin, D. Fan, J. Wang, and M. S. Triantafyllou, "Flexible cylinder flow-induced vibration", *Physics of Fluids*, 34(1), 011302, 2022. <https://doi.org/10.1063/5.0078418>.
- [2] O. A. El-Samni, "On three-dimensionality of turbulent buoyant channel flow", *Jordan Journal of Mechanical and Industrial Engineering*, 1(2), 2007, pp. 99–104.
- [3] O. M. Oyewola, O. S. Ismail, & K. Abu, "Numerical Simulation of Forced Convection Flows over a Pair of Circular Cylinders in Tandem Arrangement", *Jordan Journal of Mechanical and Industrial Engineering*, 13(4), 2019, pp. 221-230.

- [4] S. E. Elshabrawy, M. N. Hussain, & I. Janajreh, "Thermoacoustic Engine Pressure Wave: Analysis of Working Fluid Effect", *Jordan Journal of Mechanical and Industrial Engineering*, 13(4), 2019.
- [5] S. Rana, H. B. Dura, & R. Shrestha, "Control of Wake Behind an Unconfined Wedge Structure by Magnetohydrodynamics", *Jordan Journal of Mechanical and Industrial Engineering*, 15(4), 2021, pp. 347-355.
- [6] B. Su, S. He, M. Zhang, and J. Feng, "Experimental study on flow-induced vibration of a circular cylinder with a downstream square plate". *Ocean Engineering*, 247, 110768, 2022. <https://doi.org/10.1016/j.oceaneng.2022.110768>.
- [7] Guntur HL, Djanali VS, and Syaifudin A. Simulation and Dynamic System Modeling in an Elastically Supported Rigid Cylinder for Vibration Energy Harvesting. In: *Recent Advances in Renewable Energy Systems*, Springer, Singapore, 2022, pp. 61-68. [https://doi.org/10.1007/978-981-19-1581-9\\_7](https://doi.org/10.1007/978-981-19-1581-9_7).
- [8] K. Ababneh, C. A. Garris, A. M. Jawarneh, and H. Tlilan, "Investigation of the Mach number effects on fluid-to-fluid interaction in an unsteady ejector with a radial-flow diffuser", *Jordan Journal of Mechanical and Industrial Engineering*, 3(2), 2009, pp.131-140.
- [9] T. Sarpkaya, "A critical review of the intrinsic nature of vortex-induced vibrations", *Journal of Fluids and Structures*, 19(4), 2004, pp. 389-447. <https://doi.org/10.1016/j.jfluidstructs.2004.02.005>.
- [10] Blevins RD. *Flow-induced vibration*. New York: Krieger Pub Co.; 2001.
- [11] Y. Taamneh, "CFD simulations of drag and separation flow around ellipsoids", *Jordan Journal of Mechanical and Industrial Engineering*, 5(2), 2011, pp. 129-132.
- [12] Hossain, A. Rahman, J. Hossen, P. Iqbal, N. Shaari, & G. K. Sivaraj, "Drag reduction in a wing model using a bird feather like winglet", *Jordan Journal of Mechanical and Industrial Engineering*, 5(3), 2011, pp. 267-272.
- [13] T. D. AlMomani, S. C. Vigmostad, & L. A. Alzube, "A Sharp-Interface Fluid-Structure Interaction Algorithm for Modeling Red Blood Cells", *Jordan Journal of Mechanical and Industrial Engineering*, 6(2), 2012, pp. 193-198.
- [14] M. Maine, M. El Oumami, O. Bouksour, & B. Nassiri, "Study of the Effect of some Deflector's Geometry Factors on the Reduction of the Aerodynamic Drag of the Car Model", *Jordan Journal of Mechanical and Industrial Engineering*, 15(3), 2021, pp. 165-272.
- [15] Putarno, "Analisis Perbandingan Transformasi Wavelet pada Pengenalan Citra Wajah", *Jurnal Generic*, Vol.5, No. 2, 2010, pp. 15-21.
- [16] K. Alba, H. Mitra, T. Gabel, R. Ostilla Monico, F. Koeck, and D. Williams, "Investigating fluid flow through a choke valve", *Bulletin of the American Physical Society*, 2022.
- [17] Neumeister RF, Petry AP, and Möller SV. Flow-Induced Vibration in a Single Row of Cylinders With  $p/D=1.26$ . In: *Pressure Vessels and Piping Conference (Vol. 85338, p. V003T04A011)*, American Society of Mechanical Engineers, 2021, July. <https://doi.org/10.1115/PVP2021-62989>.
- [18] Neumeister RF, Petry AP, and Möller SV. Wavelet Analysis of FIV Response for Single Cylinder and Pairs of Cylinders in Tandem and Side-by-Side. In: *Pressure Vessels and Piping Conference (Vol. 58950, p. V004T04A023)*, American Society of Mechanical Engineers, 2019, July. <https://doi.org/10.1115/PVP2019-93665>.
- [19] H. Ren, M. Zhang, J. Cheng, P. Cao, Y. Xu, S. Fu, and C. Liu, "Experimental Investigation on Vortex-Induced Vibration of a Flexible Pipe under Higher Mode in an Oscillatory Flow", *Journal of Marine Science and Engineering*, 8(6), 2020, pp. 408-430. <https://doi.org/10.3390/jmse8060408>.
- [20] S. Pandian, S. L. N. Desikan, & S. Niranjana, "Nonlinear characteristics of a rectangular cavity in supersonic flow". *AIAA Journal*, 58(3), 2020, pp.1206-1215. <https://doi.org/10.2514/1.J058709>.
- [21] R. F. Neumeister, A. P. Petry, and S. V. Möller, "Experimental flow-induced vibration analysis of the crossflow past a single cylinder and pairs of cylinders in tandem and side-by-side". *Journal of Pressure Vessel Technology*, 143(3), 2021, pp. 13p. <https://doi.org/10.1115/1.4048101>.
- [22] De Moortel, S. A. Munday, and A. W. Hood, "Wavelet Analysis: the effect of varying basic wavelet parameters", *Solar Physics* 222, 2004, pp. 203-228. <https://doi.org/10.1023/B:SOLA.0000043578.01201.2d>
- [23] J. Chebil, G. Noel, M. Mesbah, & M. Deriche, "Wavelet decomposition for the detection and diagnosis of faults in rolling element bearings". *Jordan Journal of Mechanical and Industrial Engineering*, 3(4), 2009, pp. 260-267.
- [24] R. J. Zhang, W. W. Yang, & X. W. Wang, "The Reliability Analysis of Horizontal Vibration of Elevator Based on Multi-State Fuzzy Bayesian Network". *Jordan Journal of Mechanical and Industrial Engineering*, 8(1), 2014, pp. 43-49.
- [25] X. Xie, A. Ma, H. Zhao, X. Li, X., and X. Wu, "Experimental investigation and analysis on the cross-flow characteristics over inline tube bundles with  $S/D=1.875$ ", *International Journal of Heat and Mass Transfer*, 203, 123800, 2023. <https://doi.org/10.1016/j.ijheatmasstransfer.2022.123800>.
- [26] M. Ababneh, M. Salah, and K. Alwidyan, "Linearization of nonlinear dynamical systems: A comparative study", *Jordan Journal of Mechanical and Industrial Engineering*, Vol. 5, No. 6, 2011, pp. 567-571.
- [27] J. Li, "A New Trajectory Planning Method of 6-DOF Apple Picking Manipulator", *Jordan Journal of Mechanical and Industrial Engineering*, Vol. 16, No. 5, 2022, pp. 777-785.
- [28] X. Fan, Z. Wang, Y. Wang, & W. Tan, "The effect of vortices structures on the flow-induced vibration of three flexible tandem cylinders", *International Journal of Mechanical Sciences*, 192, 2021. <https://doi.org/10.1016/j.ijmecsci.2020.106132>.
- [29] Wavelet Transformation Analysis Applied To Incompressible Flow Field About A Solid Cylinder". S. Sadeqi, N. Xiros, S. Rouhi, J. Ioup, J. VanZwieten, and C. Sultan. "5-6th Thermal and Fluids Engineering Conference (TFEC)", 2021.
- [30] M. Eswaran, S. D. Sajish, K. P. Anup, K. S. Suresh, N. S. Dudala, B. K. Sreedhar, & S. Raghupathy, "Investigation of axial Flow-Induced vibration in a single fuel Sub-Assembly due to radial clearance", *Annals of Nuclear Energy*, 181, 2023. <https://doi.org/10.1016/j.anucene.2022.109546>.
- [31] W. Chen, Y. Wei, C. Ji, & Y. Zhao, "Mass ratio effects on flow-induced vibrations of an equilateral triangular prism", *Journal of Fluids and Structures*, 116, 2023. <https://doi.org/10.1016/j.jfluidstructs.2022.103808>.
- [32] L. Li, Y. Tan, W. Xu, Y. Ni, J. Yang, & D. Tan, "Fluid-induced transport dynamics and vibration patterns of multiphase vortex in the critical transition states". *International Journal of Mechanical Sciences*, 252, 2023. <https://doi.org/10.1016/j.ijmecsci.2023.108376>.
- [33] Hossain, A., P. R. Arora, A. Rahman, A. A. Jaafar, & A. P. Iqbal, "Analysis of longitudinal aerodynamic characteristics of an aircraft model with and without winglet", *Jordan Journal of Mechanical and Industrial Engineering*, Vol. 2, No. 3, 2008, pp. 143 - 150.
- [34] M. Al Zou'bi, "Renewable energy potential and characteristics in Jordan", *Jordan Journal of Mechanical and Industrial Engineering*, Vol. 4, No. 1, 2010, pp. 45-48.
- [35] O. Al-Araidah, W. Batayneh, T. Darabseh, & S. M. BaniHani, "Conceptual design of a single DOF human-like eight-bar leg

- mechanism”, Jordan Journal of Mechanical and Industrial Engineering, Vol. 5, No. 4, 2011, pp. 285-289.
- [36] F. H. Darwish, G. M. Atmeh, & Z. F. Hasan, “Design Analysis and Modeling of a General Aviation Aircraft”, Jordan Journal of Mechanical and Industrial Engineering, Vol. 6, No. 2, 2012, pp. 183 – 191.
- [37] R. Ali, & A. Singh, “Numerical Study of Fluid Dynamics and Heat Transfer Characteristics for the Flow Past a Heated Square Cylinder”, Jordan Journal of Mechanical and Industrial Engineering, Vol. 15, No. 4, 2021, pp. 357-376.
- [38] Prabhu, “Investigation on the Performance of Order Release Methods in a Flow Shop with Bottlenecks”, Jordan Journal of Mechanical and Industrial Engineering, Vol. 15, No. 4, 2021, pp. 377-385.
- [39] T. K. Sahoo, & P. Ghose, “Effect of Inlet Swirl on Combustion Performance and Soot Formation of a Turbulent Methane-Air Non-Premixed Flame”, Jordan Journal of Mechanical and Industrial Engineering, Vol. 16, No. 2, 2022, pp. 309-318.
- [40] H. Laidoudi, A. K. Hussein, A. B. Mahdi, O. Younis, E. H. Malekshah, H. Togun, & U. Biswal, “Numerical Investigation of Buoyancy-driven Flow in a Crescent-shaped Enclosure”, Jordan Journal of Mechanical and Industrial Engineering, 16(4), 2022, pp. 627-644.
- [41] Y. T. Sheen, and C. K. Hung, “Constructing a wavelet-based envelope function for vibration signal analysis”, Mechanical Systems and Signal Processing, Vol. 18, No. 1, 2004, pp. 119–126. [https://doi.org/10.1016/S0888-3270\(03\)00046-3](https://doi.org/10.1016/S0888-3270(03)00046-3).
- [42] R. Maryami, E. J. Arcondoulis, Q. Liu, & Y. Liu, “Experimental near-field analysis for flow induced noise of a structured porous-coated cylinder”, Journal of Sound and Vibration, Vol. 551, 2023. <https://doi.org/10.1016/j.jsv.2023.117611>.
- [43] P. Han, E. de Langre, M. C. Thompson, K. Hourigan, and J. Zhao, “Vortex-induced vibration forever even with high structural damping”, Journal of Fluid Mechanics, Vol. 962, 2023. <https://doi.org/10.1017/jfm.2023.268>.
- [44] J. Zhou, J. Liu, & A. Guo, “Investigation of the dynamic behavior of the flow–structure system of submerged floating tunnels under wave and current actions”, Coastal Engineering, Vol. 183, 2023. <https://doi.org/10.1016/j.coastaleng.2023.104329>.
- [45] W. Liu, H. Tang, N. N. B. Thierry, J. Zhang, F. Zhang, M. Zhu, ... & F. Hu, “The profile and fluttering characteristics of a codend with different mesh sizes and catch by fast Fourier transform and Morlet wavelet methods”, Fisheries Research, Vol. 264, 2023. <https://doi.org/10.1016/j.fishres.2023.106714>.
- [46] Y. Wang, C. He, X. Wang, H. Cheng, & B. Ji, “Influence of skew angle on the cavitation dynamics and induced low-frequency pressure fluctuations around a marine propeller”, Ocean Engineering, Vol. 277, 2023. <https://doi.org/10.1016/j.oceaneng.2023.114302>.
- [47] Y. Sun, Q. Liu, L. Shao, Y. Wang, X. Chang, & K. Liu, “Experimental investigation of aerodynamic forces and vortex-induced vibrations of wavy cylinders at subcritical Reynolds numbers”, Experimental Thermal and Fluid Science, Vol. 144, 2023. <https://doi.org/10.1016/j.expthermflusci.2023.110869>.
- [48] J. Xi, J. Wang, X. A. Si, & H. Dong, “Direct numerical simulations and flow-pressure acoustic analyses of flapping-uvula-induced flow evolutions within normal and constricted pharynx”, Theoretical and Computational Fluid Dynamics, Vol. 37, 2023, pp. 131-149. <https://doi.org/10.1007/s00162-023-00638-1>.
- [49] R. Janeliukstis, “Continuous wavelet transform-based method for enhancing estimation of wind turbine blade natural frequencies and damping for machine learning purposes”, Measurement, Vol. 172, 2021, pp. 108897. <https://doi.org/10.1016/j.measurement.2020.108897>.
- [50] Y. Wang, M. Lou, X. H. Ren, W. X. Liang, X. Li, & P. B. Andg, “Experimental Investigation of Multi-Mode Vortex-Induced Vibration of Flexible Risers with Different Mass Ratios”, China Ocean Engineering, Vol. 37, No. 1, 2023, pp. 1-15. <https://doi.org/10.1007/s13344-023-0001-y>.
- [51] Gholami, M. Amabili, & M. P. Païdoussis, “Experiments on the dynamics and stability of cantilevered circular cylindrical shells conveying airflow”, Nonlinear Dynamics, Vol. 111, No. 8, 2023, pp. 7005-7026. <https://doi.org/10.1007/s11071-023-08245-9>.
- [52] P. K. Ullas, D. Chatterjee, & S. Vengadesan, “Experimental study on the effect of throat length in the dynamics of internal unsteady cavitating flow”, Physics of Fluids, Vol. 35, No. 2, 2023. <https://doi.org/10.1063/5.0136383>.
- [53] W. J. Staszewski, “Identification of nonlinear systems using multi-scale ridges and skeletons of the wavelet transform”. Journal of Sound and Vibration, Vol. 214, No. 4, 1998, pp. 639–658. <https://doi.org/10.1006/jsvi.1998.1616>.
- [54] T. Tjahjowidodo, F. Al-Bender, and H. Van Brussel, “Experimental dynamic identification of backlash using skeleton methods”. Mechanical Systems and Signal Processing, Vol. 21, No. 2, 2007, pp. 959–972. <https://doi.org/10.1016/j.ymssp.2005.11.002>.
- [55] Hammid A, and Biantoro AW. Identifying the Nonlinearity of Structures Dynamics by Wavelet Packet Decomposition. In IOP Conference Series: Materials Science and Engineering, Vol. 453, No. 1, 2018. DOI 10.1088/1757-899X/453/1/012003.
- [56] Hamid, “The Investigation of the Effect of Heaving and Pitching on Wave-Induced Vertical Hull Vibration of a Container Ship in Regular Waves”, Journal of Mechanics Engineering and Automation, Vol. 1, No. 6, 2011, pp. 491-496.
- [57] Susanto, S. Q. Yusuf, A. Hamid, H. Wahyudi, and S. Subekti, “Implementation of frequency response function on taper bearing maintenance”, Sinergi, Vol. 23, No. 2, 2019, pp. 132-138. <http://doi.org/10.22441/sinergi.2019.2.006>.
- [58] D. Effendi, Subekti, and A. Hammid, “Karakteristikdinamik disc brake daihatsuSigra 1200 cc denganmetode bump test”, Flywheel: JurnalTeknikMesinUntirta, Vol. 5, No. 1, 2019, pp. 14-19. <http://dx.doi.org/10.36055/fwl.v0i0.3947>.
- [59] H. Sangian, D. A. Rahman, R. Rudiwanto, S. Subekti, and A. Hamid, “Analisisgetaranpada screw compressor akibatpengaruhputaran rotor”, JurnalRekayasaMesin, Vol. 11, No. 2, 2020, pp. 267-275. <https://doi.org/10.21776/ub.jrm.2020.011.02.13>.
- [60] M. A. Pratiwi, M. Ikhsan, R. D. Octavianto, A. Hamid, and S. Subekti, “Dynamic characterization of ball bearing in turbine propeller using bump testmethod”, Sinergi, Vol. 25, No. 2, 2021, pp. 135-140. <http://dx.doi.org/10.22441/sinergi.2021.2.004>.
- [61] M. F. Gulang, Z. D. Haq, H. Alpiyanto, and S. Subekti, “Karakteristikdinamik needle bearing pada camshaft dohcuzukisatria fu150 yang telah di modifikasi, denganmetode bump test”. Teknika: JurnalSainsand Teknologi, Vol. 16, No. 2, 2020, pp. 237-243. <http://dx.doi.org/10.36055/tjst.v16i2.8461>.
- [62] M. Ikhsan, and S. Subekti, “AnalisisGetaran Tapered Roller Bearing Pada Turbine Propeller Sebelumand Sesudah Pelumasan (Oli& Grease) DenganMetode Bump Test”, Barometer, Vol. 5, No. 2, 2020, pp. 277-281. DOI: 10.35261/barometer.v5i2.3764.
- [63] F. Wicaksono, and S. Subekti, “AnalisisPengaruh PenyumbatanAliranFluidapadaPipadengan Metode Fast Fourier Transform”, JurnalDinamikaVokasional TeknikMesin, Vol. 6, No. 1, 2021, pp. 77-83. DOI:10.21831/dinamika.v6i1.36339.

- [64] K. Berahmana, "Analisis Getaran Pada Aliran Pipa Akibat Pemasangan Turbine Propeller", *AME (Aplikasi Mekanika and Energi): Jurnal Ilmiah Teknik Mesin*, 7(1), 2021, pp. 9-15. <https://doi.org/10.32832/ame.v7i1.3667>.
- [65] S. M. Nacy, N. K. Alsaheb, and F. F. Mustafa, "Vibration analysis of plates with spot welded stiffeners", *Jordan Journal of Mechanical and Industrial Engineering*, Vol. 3, No. 4, 2009, pp. 272 – 279.
- [66] N. K. A. Al-Sahib, A. N. Jameel, & O. F. Abdulateef, "Investigation into the vibration characteristics and stability of a welded pipe conveying fluid", *Jordan Journal of Mechanical and Industrial Engineering*, Vol. 4, No. 3, 2010, pp. 378-387.
- [67] M. Abu-Hilal, & A. R. Touqan, "Conceptual Understanding of Mass and Stiffness Fixed Points of Discrete Vibrational Systems", *Jordan Journal of Mechanical and Industrial Engineering*, Vol. 4, No. 4, 2010, pp. 433 – 442.
- [68] M. A. Nawafleh, N. Al-Kloub, M. Tarawneh, & R. M. Younesd, "Reduction of vibration of industrial equipments", *Jordan Journal of Mechanical and Industrial Engineering*, Vol. 4, No. 4, 2010, pp. 495-502.
- [69] R. Dweiri, "The Potential of Using Graphene Nanoplatelets for Electrically Conductive Compression-Molded Plates", *Jordan Journal of Mechanical and Industrial Engineering*, Vol. 9, No. 1, 2015, pp. 1 – 8.
- [70] Z. Yu, H. Jia, & X. Huang, "Vibration Fatigue Analysis and Optimization Design of a Lighttruck Urea Box Bracket", *Jordan Journal of Mechanical and Industrial Engineering*, Vol. 14, No. 1, 2020, pp. 167 – 173.
- [71] A. Ahmed, & M. M. S. Mulapeer, "Torsional vibration of a Rod Composed of Two Dissimilar Frictionally Welded Parts with and without Crack in a Thermal Environment", *Jordan Journal of Mechanical and Industrial Engineering*, Vol. 16, No. 3, 2022, pp. 169 – 179.
- [72] J. Xi, M. Talaat, X. Si, and H. Dong, "Flow Dynamics and Acoustics from Glottal Vibrations at Different Frequencies", *In Acoustics*, Vol. 4, No. 4, 2022, pp. 915-933. <https://doi.org/10.3390/acoustics4040056>.
- [73] L. Li, P. Liu, and H. Guo, "Time-frequency characteristics of noise generated from different slat and flap geometrical configurations of the high-lift device", *Applied Acoustics*, Vol. 197, 2022, pp. 108891. <https://doi.org/10.1016/j.apacoust.2022.108891>.
- [74] P. Radomir, "Binary PSK/CPFSK and MSK band pass modulation identifier based on the complex Shannon wavelet transform", *Journal of Electrical Engineering*, Vol. 56, No. 3-4, 2005, pp. 71-77.
- [75] L. Wang, J. Zhang, C. Wang, and S. Hu, "Identification of nonlinear system through time-frequency filters technique", *Journal of Vibration and Acoustic*, Vol. 125, No. 2, 2003, pp. 199-204. <https://doi.org/10.1115/1.1545769>.
- [76] N. Özkurt, and F. A. Savaci, "Determination of wavelet ridges of nonstationary signals by singular value decomposition", *IEEE Trans. On Circuits and system*, Vol. 52, No. 8, 2005, pp. 480-485. DOI: 10.1109/TCSII.2005.849041.
- [77] Analysis and detection of forced oscillation using synchrosqueezed wavelet based ridge technique". P. Singh, A. Prakash, K. Kumar, & S. K. Parida," 2022 IEEE IAS Global Conference on Emerging Technologies (GlobConET), 2022, pp. 417-422. DOI: 10.1109/GlobConET53749.2022.9872167.
- [78] Y. Zhou, J. Ma, F. Li, B. Chen, T. Xian, & X. Wei, "An Improved Algorithm for Peak Detection Based on Weighted Continuous Wavelet Transform", *IEEE Access*, Vol. 10, 2022, pp. 118779-118788. DOI: 10.1109/ACCESS.2022.3220640.
- [79] Schmal, G. Mönke, & A. E. Granada, "Analysis of complex circadian time series data using wavelets", *In Circadian Regulation: Methods and Protocols*, New York, NY: Springer US, Vol. 2482, 2022, pp. 35-54. [https://doi.org/10.1007/978-1-0716-2249-0\\_3](https://doi.org/10.1007/978-1-0716-2249-0_3).
- [80] Tian, S. Wen, X. Li, J. Ju, J. Tang, and N. Xiong, "PFMD: A Power Frequency Magnetic Anomaly Signal Detection Scheme Based on Synchrosqueezed Wavelet Transform", *Applied Sciences*, Vol. 12, No. 21, 2022, pp. 10735. <https://doi.org/10.3390/app122110735>.
- [81] Characterization of nonlinear, nonstationary systems in operational modal analysis using wavelet transform". R. Carpine, P. Argoul, and C. Rospars", *ISMA-USD Noise and Vibration Engineering Conference 2022*, 2022,
- [82] X. Yunsong, D. M. Siringoringo, and Y. Fujino, "Condition assessment of seismically isolated multi-span highway bridge bearings using recorded and simulated seismic responses", *Advances in Structural Engineering*, Vol. 25, No.16, 2022, pp. 3299-3315. <https://doi.org/10.1177/13694332221133195>.
- [83] Y. Hu, X. Tu, F. Li, Y. Zhu, & J. Lu, "Adaptive instantaneous frequency ridge extraction based on target tracking for frequency-modulated signals", *ISA transactions*, Vol. 128, 2022, pp. 665-674. <https://doi.org/10.1016/j.isatra.2021.10.011>.
- [84] Gianni I. Modal parameter identification using the continuous wavelet transform. National Technical University of Athens: 2022.
- [85] W. Haonian, Y. Li, T. Yuyuan, and N. Xiangfan, "Method improving low Signal-to-noise ratio of velocity test signals for Laser-induced shock waves." *Optics & Laser Technology*, Vol. 155, 2022, pp. 108362. <https://doi.org/10.1016/j.optlastec.2022.108362>.
- [86] M. Siringoringo, and Y. Fujino, "Wavelet-based analysis for detection of isolation bearing malfunction in a continuous multi-span Girder Bridge", *Journal of Earthquake Engineering*, Vol. 26, No.10, 2022, pp. 5237-5267. <https://doi.org/10.1080/13632469.2020.1868363>